
Nonlinear Optics

$\chi^{(2)}$ MATERIALS

2.1 Nonlinear optics in $\chi^{(2)}$ media

In this section, we will only focus on materials which present a nonlinear susceptibility $\chi^{(2)}$. As we saw from the previous chapter, this happens in the case of the Lorentz model with an asymmetric potential. Fig. 2.1 presents the linear (blue curve) and nonlinear (red curve) response of polarization \mathbf{P} to an applied field \mathbf{E} . As a field propagates in a $\chi^{(2)}$ material, not only it will induce such polarization, but the polarization will then act back on the field itself. The modified field \mathbf{E}_{out} is also presented.

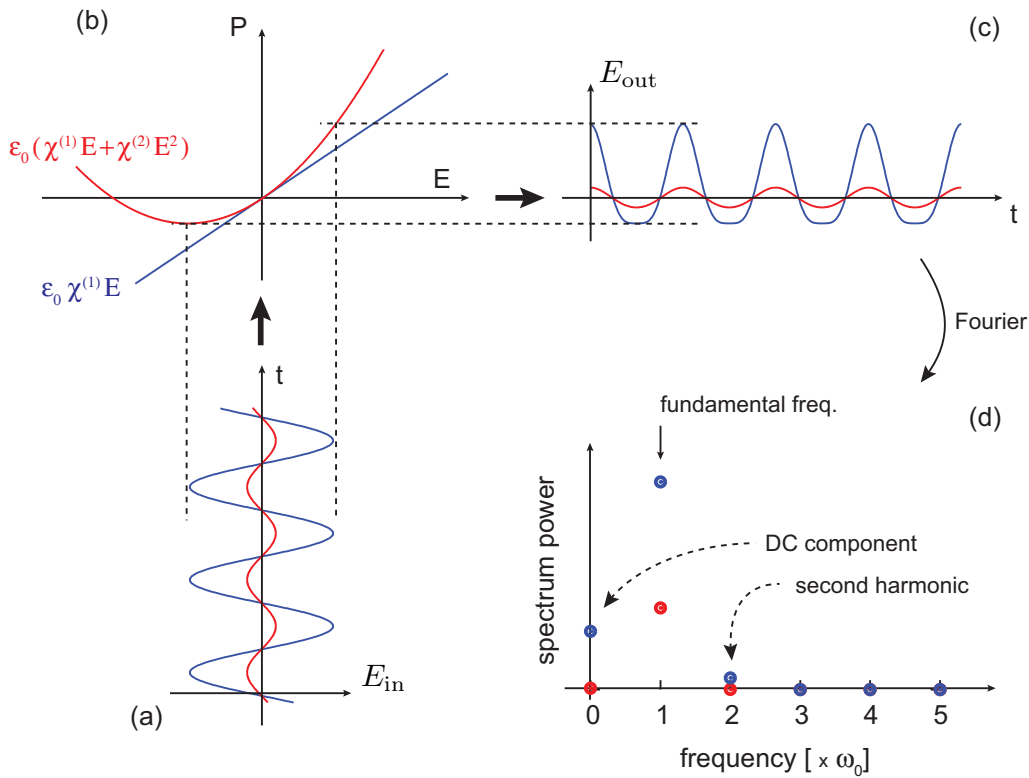


Figure 2.1: Effect of the induced polarization on the electric field for low (red) and high (blue) input power in a $\chi^{(2)}$ material. For high input power, the Fourier spectrum shows the appearance of a component at $2\omega_0$ (second harmonic) as well as a DC component.

From the power spectrum of the output field (Fig. 2.1-d), we can see that as the strength of the input field increases (blue curve), new components appear in the spectrum:

1. a DC-component
2. a component at the second harmonic

Actually, $\chi^{(2)}$ materials can be used for the following nonlinear applications:

1. three waves mixing
2. second harmonic generation
3. sum and difference frequencies generation
4. parametric oscillation

2.1.1 Frequency mixing

Let's assume that we have two fields entering a $\chi^{(2)}$ material. The field is simply the superposition of two simple electric fields:

$$E(t) = \frac{1}{2} (\mathcal{E}_1 e^{-i\omega_1 t} + c.c.) + \frac{1}{2} (\mathcal{E}_2 e^{-i\omega_2 t} + c.c.) \quad (2.1)$$

and the induced polarization:

$$P = \epsilon_0 \chi^{(2)} E(t)^2 \quad (2.2)$$

After calculation, the polarization is:

$$\begin{aligned} \frac{4P}{\epsilon_0 \chi^{(2)}} = & \mathcal{E}_1^2 e^{-2i\omega_1 t} + c.c. && \leftarrow \text{SHG of } E_1 \\ & + \mathcal{E}_2^2 e^{-2i\omega_2 t} + c.c. && \leftarrow \text{SHG of } E_2 \\ & + 2\mathcal{E}_1 \mathcal{E}_2 e^{-i(\omega_1 + \omega_2)t} + c.c. && \leftarrow \text{sum frequency } (\omega_1 + \omega_2) \\ & + 2\mathcal{E}_1 \mathcal{E}_2^* e^{-i(\omega_1 - \omega_2)t} + c.c. && \leftarrow \text{difference frequency } (\omega_1 - \omega_2) \\ & + |\mathcal{E}_1|^2 + |\mathcal{E}_2|^2 && \leftarrow \text{DC field : optical rectification} \end{aligned}$$

Of course, for each case, the input field generates a polarization, which drives the field component through Maxwell's equations. At that moment, the important question to ask is : "Will we generate all these frequencies as soon as we use 2 fields in a $\chi^{(2)}$ materials?". The answer is *fortunately no*.

2.1.2 Franken's experiment of second harmonic generation

One of the most famous paper in nonlinear optics is certainly the 1st demonstration of the generation of second harmonic in quartz by Franken, Hill, Peter and Weinreich in 1961. In this experiment, the authors used a recently demonstrated ruby laser ($\lambda_p = 0.694 \mu\text{m}$), operating in pulsed regime. The laser beam is focused into a quartz crystal and the output beam (pump & second harmonic) was dispersed with a prism and sent onto a photographic plate (fig. 2.2).

This paper is not only famous for the amazing result that was presented: it was indeed the very first time that someone could demonstrate that a coherent source (laser beam) could lead to the generation of coherent harmonics, and this was clearly an important milestones for optics.

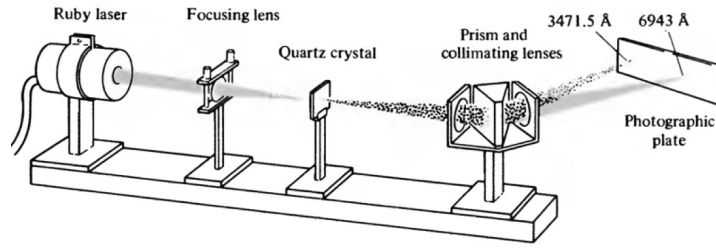


Figure 2.2: Experimental setup of the Franken's experiment of second harmonic generation.

This paper is also famous because, the result does not appear in the paper! As you can see on the copy of the main figure of that paper (fig. 2.3), published in *Physical Review letter* in 1961, the arrow, supposed to point at the second harmonic, does not point to anything! At that time, the authors could not simply send a pdf version of their paper, including high-resolution figures and check the proofs of the paper just before its publication on the web! Actually, the final stage was to go through a printer, who was preparing the new edition of PRL. But the conversion efficiency of the process was so low ($\simeq 10^{-8}$ conversion efficiency) that the result, a small point caught by the photographic plate, was considered as a simple dust by the editor, who simply erased it!

VOLUME 7, NUMBER 4

PHYSICAL REVIEW LETTERS

AUGUST 15, 1961

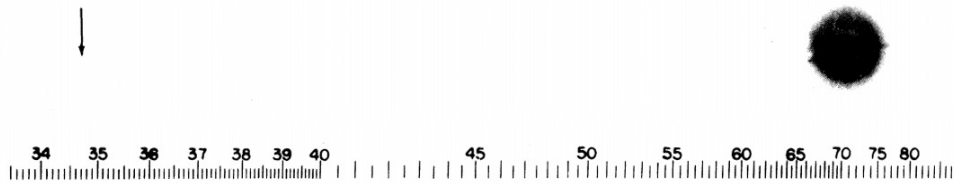


FIG. 1. A direct reproduction of the first plate in which there was an indication of second harmonic. The wavelength scale is in units of 100 Å. The arrow at 3472 Å indicates the small but dense image produced by the second harmonic. The image of the primary beam at 6943 Å is very large due to halation.

Figure 2.3: Copy of the figure from presenting the results of the second harmonic generation by the group of P. Franken in 1961.

Let's see why the conversion efficiency of the original second harmonic experiment was so small. The input field is simply

$$E_1 = \frac{1}{2} [\mathcal{E}_1 e^{-j(\omega_1 t - k_1 z)} + c.c.] \quad (2.3)$$

with

$$k_1 = n_1 \frac{\omega_1}{c} \quad (2.4)$$

where n_1 is the refractive index of the material at the frequency ω_1 , and c the velocity of light in vacuum. As we mentioned already, the input field will induce a polarization term at $\omega_2 = 2\omega_1$:

$$P[\omega_2] = \frac{1}{4} \epsilon_0 \chi^{(2)} [\mathcal{E}_1^2 e^{-j(2\omega_1 t - 2k_1 z)} + c.c.] \quad (2.5)$$

This induces a new field E_2 , which will propagate inside the crystal. This field is described as

$$E_2 = \frac{1}{2} [\mathcal{E}_2 e^{-j(\omega_2 t - k_2 z)} + c.c.] = \frac{1}{2} [\mathcal{E}_2 e^{-j(2\omega_1 t - k_2 z)} + c.c.] \quad (2.6)$$

with

$$k_2 = \frac{n_2 \omega_2}{c} = \frac{n_2 \times 2\omega_1}{c} \quad (2.7)$$

The generated field E_2 and the induced polarization at ω_2 are actually oscillating in phase if and only if the argument of the exponential functions are identical. In other words, they oscillate in phase if and only if $n_1 = n_2$. As fig. 2.4 shows, the chromatic dispersion prevents such equality¹. We can introduce a *mismatch parameter* $\Delta k = 2k_1 - k_2$ and use

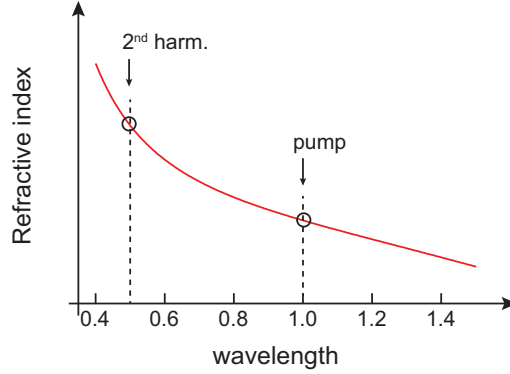


Figure 2.4: Evolution of the refractive index as a function of the wavelength.

it to write the *coherence length* ($L_{\text{coh.}}$) for second harmonic generation:

$$L_{\text{coh.}} = \frac{2\pi}{|\Delta k|} = \frac{2\pi}{\left| n_2 \frac{2\omega}{c} - 2 \frac{n_1 \omega}{c} \right|} = \frac{2\pi c}{2\omega |n_2 - n_1|} = \frac{\lambda}{2 |n_2 - n_1|} \quad (2.8)$$

In the case of Franken & co-workers experiment, the coherence length was only a few microns!

2.1.3 General case

Let's assume that the experiment now focuses on sum-frequency generation. Two fields are required

$$E = \mathcal{E}_1 e^{i(\mathbf{k}_1 \cdot \mathbf{r} - \omega_1 t)} + \mathcal{E}_2 e^{i(\mathbf{k}_2 \cdot \mathbf{r} - \omega_2 t)} + c.c. \quad (2.9)$$

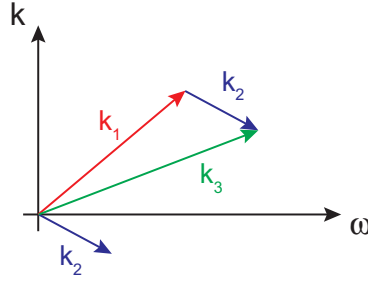
In this case, the fields are not necessarily co-linear. In the nonlinear polarization, the sum-frequency term will appear as

$$P = \epsilon_0 \chi^{(2)} [\dots + \mathcal{E}_1 \mathcal{E}_2 e^{i(\mathbf{k}_1 + \mathbf{k}_2) \cdot \mathbf{r} - (\omega_1 + \omega_2)t} + \dots] \quad (2.10)$$

For the process to be efficient, we need to fulfill 2 conditions (fig. 2.5):

$$\omega_3 = \omega_1 + \omega_2 \Rightarrow \hbar\omega_3 = \hbar\omega_1 + \hbar\omega_2 \quad (\text{conservation of energy}) \quad (2.11a)$$

$$\mathbf{k}_3 = \mathbf{k}_1 + \mathbf{k}_2 \Rightarrow \hbar\mathbf{k}_3 = \hbar\mathbf{k}_1 + \hbar\mathbf{k}_2 \quad (\text{conservation of momentum}) \quad (2.11b)$$


 Figure 2.5: k vs. ω diagram for phase-matching

Usually, phase-matching requires the use of birefringence. For linear case (for instance inside a fiber), the phase-matching condition becomes simply

$$n_3\omega_3 = n_1\omega_1 + n_2\omega_2 \quad (2.12)$$

2.2 Second harmonic generation

First, we should state that as an incident field arrives on a $\chi^{(2)}$ crystal, the induced polarization $P_{\text{NL}} = \epsilon_0\chi^{(2)}E^2$ will lead to the generation $E_{\text{in}}(\omega) \rightarrow E(2\omega)$. And as soon as this second harmonic exists and travels together with the fundamental we can have:

$$\left\{ \begin{array}{l} \omega + 2\omega \\ 2\omega - \omega \\ \omega + \omega \\ 2\omega + 2\omega \rightarrow 4\omega \\ \dots \end{array} \right.$$

Starting at one frequency $m\omega$ (with $m = 1$) leads to the combination $1 + 2$ then $1 + 2 + 3 + \dots$. And the resulting polarization, in a very general form can be written as

$$P = \sum_m \tilde{P}[m\omega] = \sum_m [P(m\omega)e^{-im\omega t} + c.c.] \quad (2.13)$$

Actually, all these higher harmonics ($m > 2$) do not need to be taken into account. This can be seen as using the *slow varying envelope approximation*: these frequencies oscillates far too fast to have any influence. In the case of second harmonic generation, where fundamental and second harmonic are co-propagating, we have the field

$$E = \mathcal{E}_1 e^{-i\omega t} + \mathcal{E}_2 e^{-2i\omega t} + c.c. \quad (2.14)$$

Then the optically induced polarization is

$$\begin{aligned} P &= \epsilon_0 [\chi^{(1)}E + \chi^{(2)}E^2] \\ &= \epsilon_0\chi^{(1)} [\mathcal{E}_1 e^{-i\omega t} + \mathcal{E}_2 e^{-2i\omega t} + c.c.] \\ &\quad + \epsilon_0\chi^{(2)} [\mathcal{E}_1^2 e^{-2i\omega t} + \cancel{\mathcal{E}_2^2 e^{-4i\omega t}} + \cancel{\mathcal{E}_1\mathcal{E}_2 e^{-3i\omega t}} + 2\mathcal{E}_1\mathcal{E}_2^* e^{i\omega t} + c.c. + |\mathcal{E}_1|^2 + |\mathcal{E}_2|^2] \end{aligned}$$

¹Realizing phase-matching will be the main topic of a separate chapter.

2.2. SECOND HARMONIC GENERATION

Therefore, we can extract the polarization term oscillating a ω and 2ω :

$$\tilde{P}_{\text{lin.}}[\omega] = \epsilon_0 \chi^{(1)} \mathcal{E}_1 e^{-i\omega t} + c.c \quad (2.15a)$$

$$\tilde{P}_{\text{lin.}}[2\omega] = \epsilon_0 \chi^{(1)} \mathcal{E}_2 e^{-2i\omega t} + c.c \quad (2.15b)$$

$$\tilde{P}_{\text{NL}}[\omega] = P(\omega) e^{-i\omega t} + c.c. = 2\epsilon_0 \chi^{(2)} \mathcal{E}_1^* \mathcal{E}_2 e^{-i\omega t} + c.c. \quad (2.15c)$$

$$\tilde{P}_{\text{NL}}[2\omega] = P(2\omega) e^{-2i\omega t} + c.c. = \epsilon_0 \chi^{(2)} \mathcal{E}_1^2 e^{-2i\omega t} + c.c. \quad (2.15d)$$

And these terms are the driving terms for the propagation equation

$$\left[\partial_{zz} - \frac{1}{c^2} \partial_{tt} \right] E = \frac{1}{\epsilon_0 c^2} \partial_{tt} P \quad (2.16)$$

Obviously, the linear term (eq. (2.15a), (2.15b)) leads to the refractive index at the fundamental and the second harmonic:

$$n_m^2 = 1 + \chi^{(1)}(m\omega) \quad (2.17)$$

Similarly, we should isolate the contributions oscillating at $e^{-i\omega t}$ and $e^{-2i\omega t}$ resulting in

$$\left[\partial_{zz} - \frac{n_m^2}{c^2} \partial_{tt} \right] E_m = \frac{1}{\epsilon_0 c^2} \partial_{tt} \tilde{P}_{\text{NL}}(m\omega) \quad \text{with } m = 1, 2 \quad (2.18)$$

Introducing the spatial dependence of the electromagnetic field

$$E_m = A_m e^{ik_m z} \quad \text{where } k_m = \frac{n_m \omega_m}{c} = \frac{n_m \times m\omega}{c} \quad (2.19)$$

and assuming that the envelope A_m varies slowly over the the length ($1/k_m$), the eq. (2.18) becomes

$$\begin{aligned} e^{ik_m z} \left[\partial_{zz} A_m + 2ik_m \partial_z A_m - \frac{n_m^2}{c^2} (\partial_{tt} A_m - 2i\omega_m \partial_t A_m) \right] \\ = \frac{1}{\epsilon_0 c^2} \left[\partial_{tt} P_{\text{NL}}(m\omega) - 2i\omega_m \partial_t P_{\text{NL}}(m\omega) - \omega_m^2 P_{\text{NL}}(m\omega) \right] \end{aligned} \quad (2.20)$$

We can then use the slow varying envelope approximation

$$\left\{ \begin{array}{l} \partial_{zz} A_m + 2ik_m \partial_z A_m \simeq 2ik_m \partial_z A_m \\ \partial_{tt} A_m - 2i\omega_m \partial_t A_m \simeq -2i\omega_m \partial_t A_m \\ \partial_{tt} P_{\text{NL}} - 2i\omega_m \partial_t P_{\text{NL}} - \omega_m^2 P_{\text{NL}} \simeq -2i\omega_m \partial_t P_{\text{NL}} - \omega_m^2 P_{\text{NL}} \simeq -\omega_m^2 P_{\text{NL}} \end{array} \right.$$

Therefore the eq. (2.20) becomes

$$e^{ik_m z} \left(2ik_m \partial_z A_m + \frac{2in_m^2 \omega_m}{c^2} \partial_t A_m \right) = -\frac{\omega_m^2}{\epsilon_0 c^2} P_{\text{NL}} \quad (2.21)$$

Using eq. (2.15c) and $m = 1$, this becomes

$$e^{ik_1 z} \left[2ik_1 \partial_z A_1 + 2i \frac{n_1}{c} k_1 \partial_t A_1 \right] = -\omega_1 \frac{2 \wp \chi^{(2)}}{\wp c^2} A_1^* A_2 e^{i(k_2 - k_1)z}$$

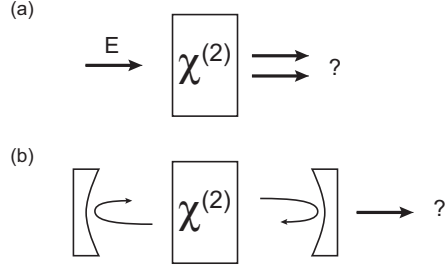


Figure 2.6: (a) free-running scheme and (b) scheme including a resonant cavity

$$\Rightarrow \boxed{\partial_z A_1 + \frac{n_1}{c} \partial_t A_1 = \frac{i\omega_1 \chi^{(2)}}{n_1 c} A_1^* A_2 e^{i(k_2 - 2k_1)z}} \quad (2.22)$$

And similarly

$$\boxed{\partial_z A_2 + \frac{n_2}{c} \partial_t A_2 = \frac{i\omega_2 \chi^{(2)}}{2 n_2 c} A_1^2 e^{-i(k_2 - 2k_1)z}} \quad (2.23)$$

At this stage, we need to distinguish between two very different situations (fig. 2.6).

In one case (fig. 2.6-a), the evolution of the pump and the generated signal happens along the crystal, but do not depend on the time. In such case the partial differentiation with respect to time $\partial_t A_m = 0$ in eq. (2.22) and (2.23) and these become a set of ordinary differential equations (eq. (2.24a), (2.24b)) In the other case, the full partial differential equations must be treated (eq. (2.22), (2.23)).

2.2.1 Free-running case

In the free-running case, the equations for the generation of second harmonic become a set of two coupled equations:

$$\frac{dA_1}{dz} = \frac{i\omega_1 \chi^{(2)}}{n_1 c} A_1^* A_2 e^{-iz\Delta k} \quad (2.24a)$$

$$\frac{dA_2}{dz} = \frac{i\omega_2 \chi^{(2)}}{2 n_2 c} A_1^2 e^{+iz\Delta k} = \frac{i\omega_1 \chi^{(2)}}{n_2 c} A_1^2 e^{+iz\Delta k} \quad (2.24b)$$

$$\text{with } \Delta k = 2k_1 - k_2$$

Obviously, the first option to deal with these equations is to solve them numerically using a good solver. This way could be simply named a *brute force approach* and usually does not really bring insight about the studied process. Looking a little closer, we can notice that

$$\begin{aligned} \frac{d|A_1|^2}{dz} &= A_1^* \frac{dA_1}{dz} + A_1 \frac{dA_1^*}{dz} = A_1^* \left[\frac{i\omega_1}{n_1 c} \chi^{(2)} A_1^* A_2 e^{-iz\Delta k} \right] + A_1 \left[\frac{-i\omega_1}{n_1 c} \chi^{(2)} A_1 A_2^* e^{iz\Delta k} \right] \\ &\Rightarrow \frac{d|A_1|^2}{dz} = \frac{i\omega_1}{n_1 c} \chi^{(2)} \left[A_1^{*2} A_2 e^{-iz\Delta k} - A_1^2 A_2^* e^{iz\Delta k} \right] \end{aligned} \quad (2.25)$$

$$\text{and for } A_2 : \frac{d|A_2|^2}{dz} = \frac{i\omega_1}{n_2 c} \chi^{(2)} \left[-A_1^{*2} A_2 e^{-iz\Delta k} + A_1^2 A_2^* e^{iz\Delta k} \right] \quad (2.26)$$

which leads to

$$n_1 \frac{d|A_1|^2}{dz} + n_2 \frac{d|A_2|^2}{dz} = 0 \quad (2.27)$$

2.2. SECOND HARMONIC GENERATION

This basically represents the conservation of the energy during the propagation. If we call J the energy flow, this quantity is constant and $n_1|A_1|^2 + n_2|A_2|^2 = J$. We can then express the amplitude of the field A_m as

$$A_m = \sqrt{\frac{J}{n_m}} \rho_m e^{i\phi_m} \quad (2.28)$$

and check that

$$\left. \begin{aligned} |A_1|^2 &= \frac{J}{n_1} \rho_1^2 \\ |A_2|^2 &= \frac{J}{n_2} \rho_2^2 \end{aligned} \right\} \Rightarrow \rho_1^2 + \rho_2^2 = 1 \quad (2.29)$$

Introducing eq. (2.28) into eq. (2.25) and (2.26) gives

$$\frac{d\rho_1}{dz} + i\rho_1 \frac{d\phi_1}{dz} = \frac{i\omega_1 \sqrt{J}}{n_1 c \sqrt{n_2}} \chi^{(2)} \rho_1 \rho_2 e^{-iz\Delta k} e^{i(\phi_2 - 2\phi_1)} \quad (2.30a)$$

$$\frac{d\rho_2}{dz} + i\rho_2 \frac{d\phi_2}{dz} = \frac{i\omega_1 \sqrt{J}}{n_1 \sqrt{n_2} c} \chi^{(2)} \rho_1^2 e^{+iz\Delta k} e^{i(2\phi_1 - \phi_2)} \quad (2.30b)$$

Since the exponential has no dimension, we can extract from these equations a characteristic length ℓ and introduce the dimensionless propagation coordinate $\zeta = z/\ell$:

$$\ell = \frac{c n_1 \sqrt{n_2}}{\omega_1 \chi^{(2)} \sqrt{J}} \quad (2.31)$$

What is important to notice is that not only this characteristic length depends on the properties of the crystal ($n_1 = n(\omega_1)$, n_2 and $\chi^{(2)}$) but also on the used energy since \sqrt{J} appears. Introducing the dimensionless propagation length $\zeta = z/\ell$ and the total phase mismatch $\theta = 2\phi_1 - \phi_2 + z\Delta k$, we get

$$\frac{d\rho_1}{d\zeta} + i\rho_1 \frac{d\phi_1}{d\zeta} = i\rho_1 \rho_2 e^{-i\theta} = i\rho_1 \rho_2 (\cos \theta - i \sin \theta) \quad (2.32a)$$

$$\frac{d\rho_2}{d\zeta} + i\rho_2 \frac{d\phi_2}{d\zeta} = i\rho_1^2 e^{i\theta} = i\rho_1^2 (\cos \theta + i \sin \theta) \quad (2.32b)$$

Separating real and imaginary parts of these equations will give the evolution of the amplitudes of each field ρ_m (real part) and total phase-mismatch (imaginary part). For the amplitudes:

$$d_\zeta \rho_1 = \rho_1 \rho_2 \sin \theta \quad (2.33a)$$

$$d_\zeta \rho_2 = -\rho_1^2 \sin \theta \quad (2.33b)$$

and since $\theta = 2\phi_1 - \phi_2 + z\Delta k$, then² $d_\zeta \theta = 2d_\zeta \phi_1 - d_\zeta \phi_2 + \ell \Delta k$. And $d_\zeta \phi_m$ are given by the imaginary parts of the eq. (2.32a), and (2.32b):

$$\left\{ \begin{aligned} \rho_1 d_\zeta \phi_1 &= \rho_1 \rho_2 \cos \theta & \Rightarrow & d_\zeta \phi_1 = \rho_2 \cos \theta \\ \rho_2 d_\zeta \phi_2 &= \rho_1^2 \cos \theta & \Rightarrow & d_\zeta \phi_2 = \left(\frac{\rho_1^2}{\rho_2} \right) \cos \theta \end{aligned} \right.$$

²Remember that $\zeta = z/\ell$ and therefore $dz/d\zeta = \ell$!

And finally:

$$\frac{d\rho_1}{d\zeta} = \rho_1\rho_2 \sin \theta \quad (2.34a)$$

$$\frac{d\rho_2}{d\zeta} = -\rho_1^2 \sin \theta \quad (2.34b)$$

$$\frac{d\theta}{d\zeta} = \left(2\rho_2 - \frac{\rho_1^2}{\rho_2}\right) \cos \theta + \ell\Delta k \quad (2.34c)$$

2.2.2 Phase-matching or not...?

It is clear from the set of equations (eq. (2.34)) that a few cases must be looked at, especially depending of the value of Δk .

Perfect phase-matching – $\Delta k = 0$

From the evolution of the phase θ , we can notice (see exercise):

$$\frac{d\theta}{d\zeta} = \left(2\rho_2 - \frac{\rho_1^2}{\rho_2}\right) \cos \theta \iff \frac{d}{d\zeta} [\ln(\rho_1^2\rho_2) \cos \theta] = 0 \quad (2.35)$$

From Eq. (2.35), we find a second invariant

$$\rho_1^2\rho_2 \cos \theta = G \quad (2.36)$$

Where G is a constant. G can either be null or not. For G to vanish, we have three cases:

(i) $\rho_1 = 0$ (ii) $\rho_2 = 0$ or (iii) $\cos \theta = 0$.

- if $\rho_1 = 0$, then $\rho_2 = 1$ (because of eq. (2.29)). This would mean that only the second harmonic signal is at the entrance of the crystal. This would correspond to another process than second harmonic generation, since the conversion will now be from $2\omega \rightarrow \omega$, which is one form of *parametric down conversion*.
- if $\rho_2 = 0$, then all the energy at the entrance of the crystal is in the fundamental frequency ($\rho_1 = 1$). The evolution of ρ_2 requires that $\sin \theta < 0$ (see eq. (2.33b)), otherwise ρ_2 would decrease and become negative, which is not physical.
- if $\cos \theta = 0$... well, this will need to be looked at more carefully.

Imperfect phase-matching – $\Delta k \neq 0$

In the case of non-perfect phase-matching, and considering that $\rho_1^2\rho_2 \cos \theta = G$ is a constant, we can notice that

$$\frac{d\theta}{d\zeta} = \left(2\rho_2 - \frac{\rho_1^2}{\rho_2}\right) \cos \theta + \ell\Delta k \iff \frac{d}{d\zeta} \left(\rho_1^2\rho_2 \cos \theta - \frac{\ell\Delta k}{2}\rho_2^2 \right) = 0 \quad (2.37)$$

And therefore, as previously, we find another *invariant*

$$\rho_1^2\rho_2 \cos \theta - \frac{\ell\Delta k}{2}\rho_2^2 = H \quad (2.38)$$

which is obviously equal to G in the case of perfect phase-matching $\Delta k = 0$. Finally, we have only three possibilities, that can lead to a non-null second harmonic generation:

- $\Delta k = 0$ and $G = 0$: we have perfect phase-matching.
- $\Delta k = 0$ and $G \neq 0$: there is already second harmonic at the entrance of the crystal. This is a seeded situation.
- $\Delta k \neq 0$

2.2.3 Perfect phase-matching and $G = 0$

The condition $G = 0$ requires $\cos \theta = 0$ and therefore $\theta = \pm\pi/2$. As discussed previously, for the second harmonic signal to grow, we must take $\sin \theta < 0$, and therefore must choose $\theta = -\pi/2$. The coupled equation (eq. (2.34)) then become:

$$\frac{d\rho_1}{d\zeta} = -\rho_1\rho_2 \quad (2.39a)$$

$$\frac{d\rho_2}{d\zeta} = +\rho_1^2 = 1 - \rho_2^2 \quad (2.39b)$$

Solution of eq. (2.39b) is simply $\tanh(\zeta + \zeta_0)$, which leads to $\rho_1(\zeta) = \text{sech}(\zeta + \zeta_0)$. And to fix the initial condition, we can impose $\rho_2(\zeta = 0) = 0$, which immediately gives the solution

$$\rho_1(\zeta) = \text{sech}(\zeta), \quad \rho_2(\zeta) = \tanh(\zeta) \quad (2.40)$$

Remember that $\zeta = z/\ell$ and

$$\ell = \frac{n_1\sqrt{n_2}}{\omega_1\chi^{(2)}} \frac{c}{\sqrt{J}} = \frac{\sqrt{n_1n_2}}{\omega_1\chi^{(2)}} \frac{\epsilon_0 c}{|A_1(z=0)|}$$

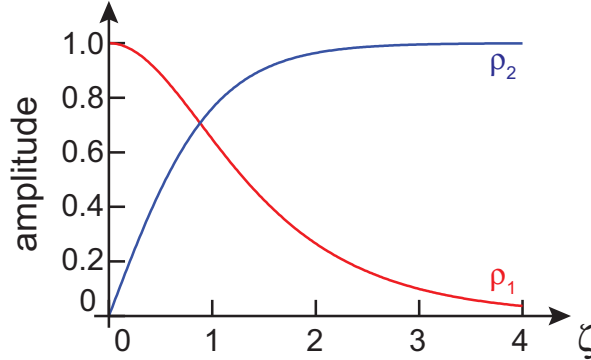


Figure 2.7: Evolution of the amplitude of the respectively the pump ρ_1 and the second harmonic ρ_2 as they are propagating inside the crystal. Initial condition is $\rho_1 = 1$, $\rho_2 = 0$, and $\theta = -\pi/2$ ($G = 0$).

From the non-dimensionless variables, we can extract the conversion efficiency of the second harmonic process:

$$\eta\left(\frac{z}{\ell}\right) = \left|\frac{A_2(z)}{A_1(0)}\right|^2 = \frac{(J/n_2)\rho_2^2(z/\ell)}{(J/n_1) \times 1} = \frac{n_1}{n_2} \tanh^2\left(\frac{z}{\ell}\right) \quad (2.41)$$

As we can see from this equation, it is not necessary to increase the propagation length inside a crystal to get a better conversion efficiency.

2.2.4 Perfect phase-matching but $G \neq 0$

Since $\rho_1^2 \rho_2 \cos \theta = G$ and $\rho_1^2 + \rho_2^2 = 1$ then

$$\cos \theta = \frac{G}{\rho_1^2 \rho_2} = \frac{G}{\rho_2 (1 - \rho_2^2)} \quad (2.42)$$

Since $d_\zeta \rho_2^2 = 2\rho_2 d_\zeta \rho_2$, and using the evolution of ρ_2 (eq. (2.34b)) then

$$\frac{d\rho_2^2}{d\zeta} = +2\rho_2 (-\rho_1 \sin \theta) = \pm 2\rho_2 \rho_1^2 \sqrt{1 - \cos^2 \theta} \quad (2.43)$$

Inserting eq. (2.42) leads to the evolution of the intensity of the second harmonic ρ_2^2 :

$$\frac{d\rho_2^2}{d\zeta} = \pm 2\rho_2 (1 - \rho_2^2) \sqrt{1 - \frac{G^2}{\rho_2^2 (1 - \rho_2^2)^2}} = \pm 2\sqrt{\rho_2^2 (1 - \rho_2^2)^2 - G^2} \quad (2.44)$$

Such equation has a solution in terms of the Jacobi elliptic functions. The main point here is that the field amplitudes ρ_1 and ρ_2 will evolve periodically along the propagation.

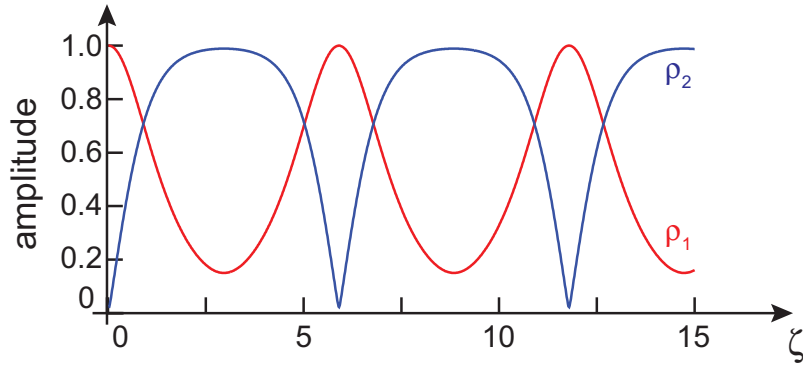


Figure 2.8: Evolution of the amplitude of the pump (ρ_1) and the second harmonic (ρ_2) as they are propagating inside the nonlinear crystal.

The two other parameters that we can modify are respectively the amount of pump (ρ_1) and the initial condition on the phase. Fig. 2.9 presents the evolution of the intensity of the second harmonic as a function of the initial parameters, respectively the input pump for a fixed phase (fig. 2.9.a), and the influence of the input phase for a fixed input pump energy.

2.2.5 Imperfect phase-matching

As we did previously, using the conservation of energy $\rho_1^2 + \rho_2^2 = 1$ and the invariant H (eq. (2.38)) we can derive the evolution of the intensity along the propagation:

$$\frac{d\rho_2^2}{d\zeta} = \pm 2\rho_2 (1 - \rho_2^2) \sqrt{1 - \cos^2 \theta} = \pm 2\sqrt{\rho_2^2 (1 - \rho_2^2)^2 - \left(H + \frac{1}{2}\ell\Delta k\rho_2^2\right)^2} \quad (2.45)$$

As before, and although the increased degree of complexity of the equation, the solution could also be expressed in terms of Jacobi elliptic function. The evolution of pump and second harmonic are, as previously, periodically changing along the propagation.

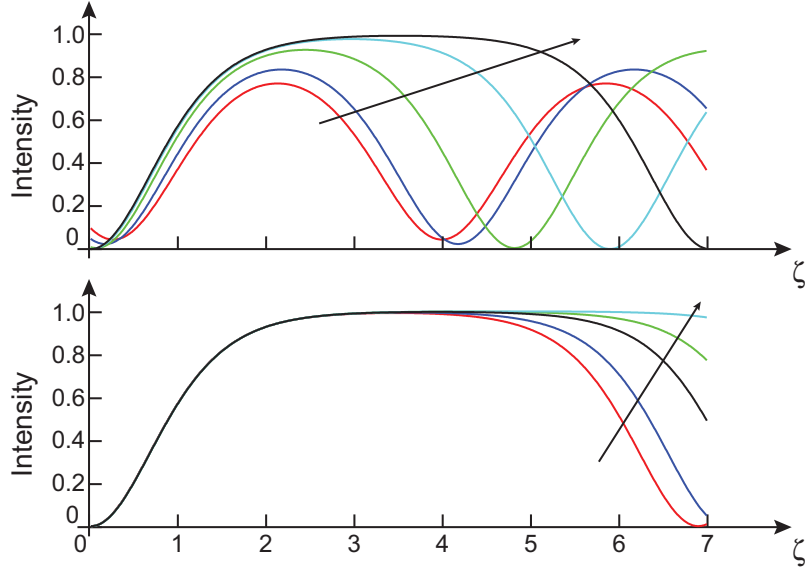


Figure 2.9: Evolution of the intensity second harmonic (ρ_2^2) for a fixed pump power as a function of the initial pump amplitude (a) and the initial phase condition (b). For (a), the initial conditions are $\theta = \pi/4$ and $\rho_1 = 0.9, 0.95, 0.99$ and 0.999 (increase as the arrow) and for (b) $\rho_1^2(0) = 0.9999$ and $\theta = 2\pi/10, 3\pi/10, 4\pi/10, 4.4\pi/10$ and $4.8\pi/10$.

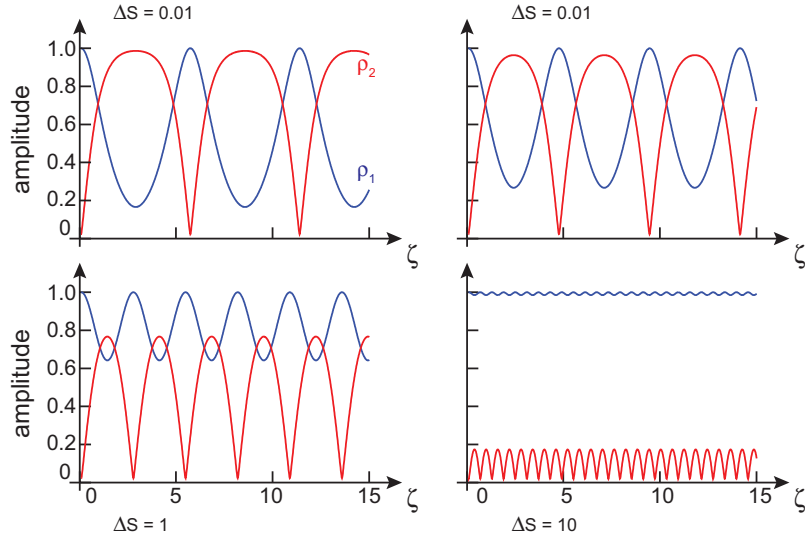


Figure 2.10: Evolution of the amplitudes (ρ_1 and ρ_2) as a function of the phase mismatch $\Delta S = \ell \Delta k$. Input conditions are $\rho_1^2(0) = 0.99$ and $\theta = \pi/4$.

It is clear that fulfilling the phase-matching conditions is a crucial point to achieve a good conversion from the pump to the second harmonic. From two fields, we saw (see. p.2) that several different combinations can lead to different new frequency, each of them requiring a specific phase-matching. What was applied here in the specific case of second harmonic generation could also be transposed to any of these cases (sum-frequency, difference frequency... etc).

2.2.6 Low depletion case

Let consider that the limit case when the pump is weakly depleted. The evolution of the second harmonic is them simply given by

$$\begin{aligned} \frac{dA_2}{dz} &= \frac{i\omega_1}{n_2c} \chi^{(2)} A_1^2 e^{iz \cdot \Delta k} \\ \Rightarrow A_2(z) &= \frac{\omega_1}{n_2c} \chi^{(2)} A_1^2 \frac{e^{iz \cdot \Delta k} - 1}{\Delta k} \quad \left(\times \frac{z}{z} \right) \end{aligned}$$

and therefore the intensity evolves as

$$|A_2(z)|^2 = \left[\frac{\omega_1 \chi^{(2)}}{n_2c} z \right]^2 |A_1|^4 \left[\frac{\sin(z \cdot \Delta k/2)}{(z \cdot \Delta k/2)} \right]^2 \quad (2.46)$$

Since the intensity if linked to the amplitude of the electric field by

$$I_i = \frac{1}{2} n_i c \epsilon_0 |A_i|^2 \quad (2.47)$$

we can rewrite eq. (2.46) as

$$\begin{aligned} I_2 &= \frac{1}{2} n_2 c \epsilon_0 \left[\frac{\omega_1 \chi^{(2)}}{n_2c} z \right]^2 \times \frac{4}{n_1^2 c^2 \epsilon^2} |I_1|^2 \operatorname{sinc}^2 \left(\frac{z \cdot \Delta k}{2} \right) \\ \Rightarrow & \boxed{I_2(z) = \frac{2 (\omega_1 \chi^{(2)})^2}{n_1^2 n_2 c^3 \epsilon_0} z^2 I_1^2 \operatorname{sinc}^2 \left(\frac{z \cdot \Delta k}{2} \right)} \quad (2.48) \end{aligned}$$

Since the *sinc* function has its maximum at $z \cdot \Delta k = 0$, and minima periodically spread at $(z \cdot \Delta k/2) = p\pi$ with $p \in \mathbb{Z}^*$. The first minimum of this function ($z \cdot \Delta k = 2p\pi$) corresponds to the coherence length:

$$z = \frac{2\pi}{\Delta k} = L_{\text{coh.}} \quad (2.49)$$

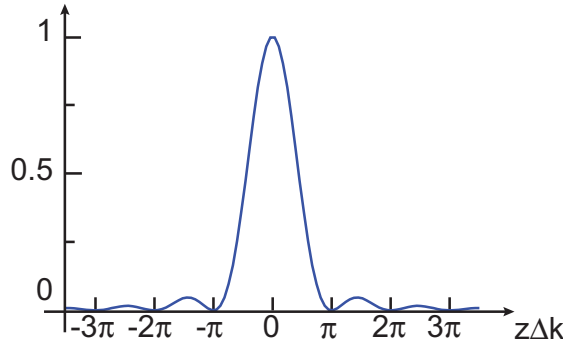


Figure 2.11: Sine cardinal and its first zeros.

Finally, from eq. (2.46) we can deduce the conversion efficiency:

$$\eta(z) = \left| \frac{A_2(z)}{A_1(0)} \right|^2 = \left(\frac{z\omega_1}{n_2c} \chi^{(2)} |A_1(0)| \right)^2 \operatorname{sinc}^2 \left(\frac{z\Delta k}{2} \right) \quad (2.50)$$

If we work at the phase-matching ($z\Delta k = 0$), then the sine cardinal is simply one, and we see that the conversion efficiency $\eta \propto |A_1(0)|^2$. Note also that the conversion efficiency increases with ω_1 : it is easier to achieve second harmonic in the visible than in the infrared!

For perfect phase-matching ($\Delta k = 0$) the conversion efficiency scales as z^2 . By contrast, when phase-matching is not fulfilled the conversion efficiency periodically oscillate (fig.). We have not discussed yet how to achieve phase-matching, but since we are using $\chi^{(2)}$ material, which are non-centrosymmetric crystal, we can imagine to grow one type of nonlinear crystal over one coherence length, and then another type (with reverse sign of Δk) so that the conversion efficiency carries on increasing along the propagation length. This idea of reversing the orientation of the crystal every coherence length is called *quasi-phase-matching* (QPM).

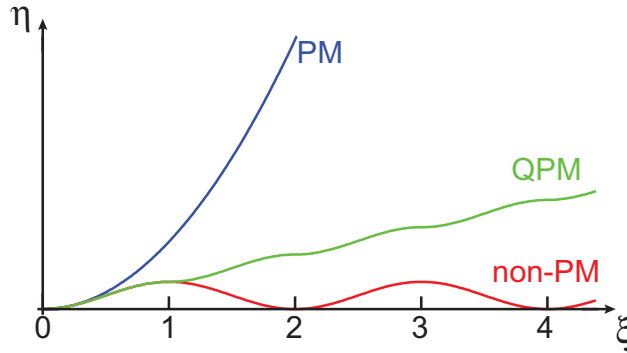


Figure 2.12: Conversion efficiency (η) of the second harmonic process for non-phase-matched (red), perfectly phase-matched (blue) and quasi-phase-matched (green) conditions as a function of the length $\xi = z/L_{\text{coh}}$.

2.2.7 Three waves mixing – Generalization

The natural generalization of second harmonic process is the sum-frequency generation: two fields oscillating respectively at ω_1 and ω_2 interact inside a $\chi^{(2)}$ crystal to generate a third wave oscillating at $\omega_3 = \omega_1 + \omega_2$. The total field inside the medium is a superposition of the three waves:

$$E(t) = \frac{1}{2} (\mathcal{E}_1 e^{-i\omega_1 t} + \mathcal{E}_2 e^{-i\omega_2 t} + \mathcal{E}_3 e^{-i\omega_3 t} + c.c.)$$

As for the case of second harmonic, we should (i) calculate the nonlinear polarization $P_{\text{NL}} = \epsilon_0 \chi^{(2)} E^2$ and then introduce it into the propagation equation

$$\partial_{zz} E_m - \frac{n_m^2}{c^2} \partial_{tt} E_m = \frac{1}{\epsilon_0 c^2} \partial_{tt} P(m\omega)$$

Using similar approach than for the second harmonic process, we can then derive the set of coupled equations:

$$\left\{ \begin{array}{l} \left(\partial_z + \frac{n_1}{c} \partial_t \right) A_1 = \frac{i\omega_1}{n_1 c} \chi^{(2)} A_2^* A_3 e^{iz\Delta k} \\ \left(\partial_z + \frac{n_2}{c} \partial_t \right) A_2 = \frac{i\omega_2}{n_2 c} \chi^{(2)} A_1^* A_3 e^{iz\Delta k} \\ \left(\partial_z + \frac{n_3}{c} \partial_t \right) A_3 = \frac{i\omega_3}{n_3 c} \chi^{(2)} A_1 A_2 e^{-iz\Delta k} \\ \Delta k = k_3 - k_1 - k_2 \end{array} \right. \quad (2.51)$$

and in the case of free-running situation (no cavity), $\partial_t A_i = 0$. Therefore we have

$$\left\{ \begin{array}{l} \frac{dA_1}{dz} = \frac{i\omega_1}{n_1 c} \chi^{(2)} A_2^* A_3 e^{iz\Delta k} \\ \frac{dA_2}{dz} = \frac{i\omega_2}{n_2 c} \chi^{(2)} A_1^* A_3 e^{iz\Delta k} \\ \frac{dA_3}{dz} = \frac{i\omega_3}{n_3 c} \chi^{(2)} A_1 A_2 e^{-iz\Delta k} \end{array} \right. \quad (2.52)$$

As previously, we can use $n_1 d_z |A_1|^2 = n_1 (A_1 d_z A_1^* + A_1^* d_z A_1)$, then

$$\left\{ \begin{array}{l} n_1 \frac{d|A_1|^2}{dz} = \omega_1 \frac{i\chi^{(2)}}{c} (A_1^* A_2^* A_3 e^{iz\Delta k} - A_1 A_2 A_3^* e^{-iz\Delta k}) \\ n_2 \frac{d|A_2|^2}{dz} = \omega_2 \frac{i\chi^{(2)}}{c} (A_1^* A_2^* A_3 e^{iz\Delta k} - A_1 A_2 A_3^* e^{-iz\Delta k}) \\ n_3 \frac{d|A_3|^2}{dz} = -\omega_3 \underbrace{\frac{i\chi^{(2)}}{c} (A_1^* A_2^* A_3 e^{iz\Delta k} - A_1 A_2 A_3^* e^{-iz\Delta k})}_{\varphi} \end{array} \right. \quad (2.53)$$

Since $\omega_1 + \omega_2 = \omega_3$, we see that

$$\begin{aligned} n_1 d_z |A_1|^2 + n_2 d_z |A_2|^2 &= -n_3 d_z |A_3|^2 \\ \Rightarrow d_z (n_1 |A_1|^2 + n_2 |A_2|^2 + n_3 |A_3|^2) &= 0 \end{aligned} \quad (2.54)$$

As for the second harmonic process we find that the conservation of energy leads to $n_1 |A_1|^2 + n_2 |A_2|^2 + n_3 |A_3|^2 = J$, where J is a constant. We can also notice from eq. (2.53) that $\varphi = (n_1/\omega_1) d_z |A_1|^2 = (n_2/\omega_2) d_z |A_2|^2 = -(n_3/\omega_3) d_z |A_3|^2$. As previously, we can use the complex notation for the amplitude

$$A_m = \sqrt{J \frac{\omega_m}{n_m}} \rho_m e^{i\phi_m} \quad (2.55)$$

and notice that

$$\begin{aligned} d_z \left(\frac{n_1}{\omega_1} |A_1|^2 - \frac{n_2}{\omega_2} |A_2|^2 \right) &= 0 = d_z J_1 \\ d_z \left(\frac{n_2}{\omega_2} |A_2|^2 + \frac{n_3}{\omega_3} |A_3|^2 \right) &= 0 = d_z J_2 \\ d_z \left(\frac{n_1}{\omega_1} |A_1|^2 + \frac{n_3}{\omega_3} |A_3|^2 \right) &= 0 = d_z J_3 \end{aligned}$$

Therefore

$$\begin{aligned} J_1 &= \frac{n_1}{\omega_1} |A_1|^2 - \frac{n_2}{\omega_2} |A_2|^2 \\ \Rightarrow J_1 &= \frac{n_1}{\omega_1} \left(J \frac{\omega_1}{n_1} \rho_1^2 \right) - \frac{n_2}{\omega_2} \left(J \frac{\omega_2}{n_2} \rho_2^2 \right) \\ \Rightarrow \frac{J_1}{J} &= \rho_1^2 - \rho_2^2 \quad \text{is invariant} \end{aligned}$$

Similarly, $\rho_1^2 + \rho_3^2 = J_3/J$ and $\rho_2^2 + \rho_3^2 = J_2/J$.

Using the definition of the amplitude A_m in the set of equations (eq. (2.53)) then leads to the generalized set of coupled equations for three wave interaction:

$$\boxed{\frac{d\rho_1}{d\zeta} = -\rho_2\rho_3 \sin \theta} \quad (2.56a)$$

$$\boxed{\frac{d\rho_2}{d\zeta} = -\rho_3\rho_1 \sin \theta} \quad (2.56b)$$

$$\boxed{\frac{d\rho_3}{d\zeta} = \rho_1\rho_2 \sin \theta} \quad (2.56c)$$

$$(2.56d)$$

where the phase $\theta = \phi_3 - \phi_1 - \phi_2 + z\Delta k$ satisfies the equation

$$\frac{d\theta}{d\zeta} = \left(\frac{\rho_1\rho_2}{\rho_3} - \frac{\rho_1\rho_3}{\rho_2} - \frac{\rho_2\rho_3}{\rho_1} \right) \cos \theta + \ell\Delta k \quad (2.57)$$

We can notice that if we are in the degenerate case, where $E_1 = E_2$ ($\rho_1 = \rho_2$), we find immediately the equations for the second harmonic (eq. (2.34)).